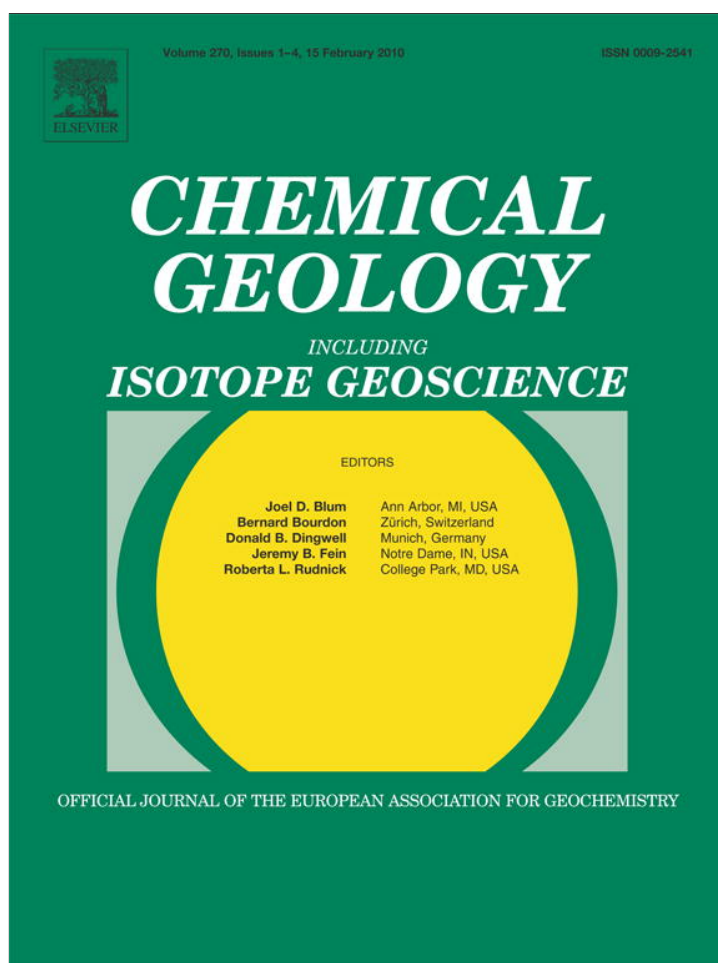


Provided for non-commercial research and education use.
Not for reproduction, distribution or commercial use.



This article appeared in a journal published by Elsevier. The attached copy is furnished to the author for internal non-commercial research and education use, including for instruction at the authors institution and sharing with colleagues.

Other uses, including reproduction and distribution, or selling or licensing copies, or posting to personal, institutional or third party websites are prohibited.

In most cases authors are permitted to post their version of the article (e.g. in Word or Tex form) to their personal website or institutional repository. Authors requiring further information regarding Elsevier's archiving and manuscript policies are encouraged to visit:

<http://www.elsevier.com/copyright>



Contents lists available at ScienceDirect

Chemical Geology

journal homepage: www.elsevier.com/locate/chemgeo

Cadmium adsorption to mixtures of soil components: Testing the component additivity approach

Daniel S. Alessi^{*}, Jeremy B. Fein

Department of Civil Engineering and Geological Sciences, University of Notre Dame, 156 Fitzpatrick Hall Notre Dame, IN 46556, United States

ARTICLE INFO

Article history:

Received 24 July 2009

Received in revised form 22 October 2009

Accepted 24 November 2009

Editor: D.B. Dingwell

Keywords:

Component additivity

Surface complexation

Cadmium adsorption

Hydrous ferric oxide

Bacillus subtilis

Kaolinite clay

ABSTRACT

The ability to predict the distribution of metals in geologic systems requires a modeling approach that can describe the competition among adsorbing surfaces for the metal of interest. In this study, we test if a component additivity (CA) surface complexation approach can account for the distribution of Cd(II) in mixtures of kaolinite, *Bacillus subtilis* bacterial cells, iron oxyhydroxide, and a dissolved organic ligand, acetate. We use existing surface complexation models to define the stoichiometries, acidity constants, and site concentrations for the important surface species on each of the sorbents, and we conduct Cd adsorption experiments with each sorbent individually to determine the stability constants for the important Cd–surface complexes on each sorbent. We test the CA approach by comparing CA predictions to measured extents of Cd adsorption in two-, three-, and four-component mixtures of the sorbents at various ratios. Our results indicate that for systems containing *B. subtilis*, iron oxyhydroxide, and kaolinite, the CA approach is a reasonable predictor of metal distribution, with the accuracy limited by the accuracy of the stability constants of the important surface complexes. However, in systems including acetate, the CA predictions significantly underestimate the extent of adsorption above pH 5, likely due to the formation of ternary Cd–acetate surface complexes on each surface. Metal-organic-surface ternary complexation and site blockage of one sorbent by another are two possible limitations of the applicability of CA surface complexation models to realistic geologic systems.

© 2009 Elsevier B.V. All rights reserved.

1. Introduction

The fate of heavy metals in soils and aquifers can be controlled by their adsorption to solid components (e.g., Meng and Letterman, 1996; Ledin et al., 1997, 1999; Covelo et al., 2007; Lund et al., 2008), aqueous complexation with dissolved organic ligands (e.g., Liu and Gonzales, 1999; Buerge-Weirich et al., 2003), and the formation of ternary surface complexes (e.g., Zachara et al., 1994; Ali and Dzombak, 1996; Fein, 2002). Although metal adsorption in multi-sorbent systems has been studied (e.g., Krantz-Rulcker et al., 1996; Ledin et al., 1997, 1999; Fingler et al., 2004; Lumsdon, 2004; Covelo et al., 2007; Landry et al., 2009; Serrano et al., 2009), the application of a quantitative surface complexation model (SCM) approach to predict metal distribution among mixtures of geosorbents is complex and difficult (Davis et al., 1998). However, the SCM approach has distinct advantages to empirical models in that the models can be extrapolated to systems of different ionic strength, pH, and component compositions (Bethke and Brady, 2000; Koretsky, 2000).

Two approaches can be used when applying SCMs to describe metal distribution in multi-sorbent systems: the component additivity (CA) approach and the general composite (GC) approach. The CA approach predicts the extent of adsorption in mixed systems based on the adsorption affinities of each solute–sorbent combination measured in isolated binary experiments, and the relative concentrations of sorption sites of each sorbent. Success of the CA approach requires that sorbents do not interact with each other, that all solutes in the system have access to all surfaces, and that the only surface complexes that form are those that form in single sorbent, single component systems as well. Previous applications of the CA approach have met with varying degrees of success. For example, Davis et al. (1998) attempted to use a SCM to predict Zn(II) adsorption onto a natural, well-characterized sedimentary mineral assemblage. The CA approach under-predicted Zn(II) uptake, likely due to difficulties in determining absolute site concentrations for each site type within the complex sediment studied. Davis et al. (1998) also applied the generalized composite (GC) approach, a semi-empirical method that assigns generic functional groups to the mineral mixture. The GC approach was more successful in modeling Zn adsorption behavior onto the sediment, but this approach is not predictive, and can only be applied to systems for which laboratory calibration exists. Kulczycki et al. (2005) found that Pb and Cd adsorption onto two-component systems comprised of ferrihydrite and either *Bacillus subtilis* or

^{*} Corresponding author. École Polytechnique Fédérale de Lausanne (EPFL), Environmental Microbiology Laboratory (EML), CE 1 543 (Centre Est), Station 6, CH-1015 Lausanne, Switzerland. Tel.: +41 21 693 63 96; fax: +41 21 693 62 05.
E-mail address: daniel.alessi@epfl.ch (D.S. Alessi).

Escherichia coli bacterial cells was less than what would be expected by summing the metal adsorption to each component determined in one-component experiments. The authors speculated that adhesion between the ferrihydrite and the bacteria masked some of the surface sites on these sorbents, decreasing the adsorption capacity of the mixture.

Several authors have successfully applied SCM models to mixtures of minerals or bacteria, in some cases with dissolved organic ligands present in the systems. For example, Pagnanelli et al. (2006) measured the adsorption of protons and Pb to quartz, muscovite, clinocllore, goethite, and hematite, individually, using a non-electrostatic SCM. They found that a component additivity SCM, using the acidity and equilibrium constants determined for each pure mineral phase, could successfully predict Pb distribution in mixtures of these solids. Fowle and Fein (1999) demonstrated that the CA approach can be successful in predicting metal adsorption to mixtures of *Bacillus licheniformis* and *B. subtilis* bacterial cells. Additionally, Yee and Fein (2003) showed that Cd, Co, Sr, and Zn adsorption onto complex mixtures of 10 species of Gram-negative and Gram-positive bacteria can be predicted with the CA approach. Lund et al. (2008) used a component additivity approach, with a diffuse layer model (DLM) to account for electric field effects, to predict the adsorption of Cu onto mixtures of hydrous ferric oxide (HFO) and kaolinite. The goodness-of-fits of the models to the experimental data were dependent on the model fits to the HFO and kaolinite individually. For mixtures of HFO and kaolinite, the authors postulated that interactions between these solids did not significantly impact Cu adsorption.

Although some tests of the CA approach have been conducted, few have tested its ability to account for metal distributions in systems containing both bacteria and minerals. Applying the CA approach to mixtures of minerals and bacteria may be problematic because bacteria can adhere to mineral surfaces, blocking reactive sites on the bacteria and the mineral (Lower et al., 2001; Ams et al., 2004). In this study, we test the ability of the CA approach to predict metal adsorption behavior in systems that contain mixtures of common soil components: kaolinite, hydrous ferric oxide (HFO), *B. subtilis* bacterial cells, and acetate as a representative simple dissolved organic acid. We use literature values to describe the proton reactivity and site concentrations for each sorbent, and we calibrate the model by measuring Cd adsorption onto each sorbent separately, using the results to calculate stability constants for the Cd–surface complexes. We use these stability constants to predict the distribution of Cd in systems with varying concentrations of each of the sorbents, and in the presence and absence of dissolved acetate. We compare these predictions to the observed extents of adsorption for these systems to test the validity of the CA approach.

2. Methods

2.1. Preparation of bacterial cells

B. subtilis, a Gram-positive soil bacterium, was selected as the biosorbent. The cell wall of this species is well-characterized (e.g., Beveridge, 1989) and the acidity constants and site concentrations of surface functional groups are well-constrained (Fein et al., 1997, 2005). The bacteria were grown and harvested in a manner similar to that described by Borrok et al. (2004). The bacteria were initially grown on agar slants made of 0.5% yeast extract and trypticase soy agar. Cells from the slant were transferred to a 3 ml test tube containing trypticase soy broth (TSB) and 0.5% yeast extract, and allowed to grow for 24 h at 32 °C. After the growth period, bacteria were transferred to 1 l solutions of the same composition, and allowed to grow for another 24 h at 32 °C. Bacteria were harvested in the stationary phase by centrifuging the broth at 9000 g for 10 min to pellet the bacteria. After decanting the broth, the bacteria were washed four times in 0.1 M NaClO₄ solutions. Between each wash, the bacteria were centrifuged at 8100 g for 5 min to

pellet the bacteria, the supernatant was decanted, and the cells were suspended in a fresh 0.1 M NaClO₄ electrolyte. After the washing cycles, the bacteria were transferred to a weighed centrifuge tube after the final wash, and centrifuged one time for 4 min and two times for 30 min at 8100 g, decanting the remaining supernatant each time. The resulting wet weight of the *B. subtilis* bacterial pellet is approximately 5 times the dry weight (Borrok et al., 2004). The method of preparation described here removes excess growth media and adsorbed cations from the bacterial surface, and renders the bacteria alive, but metabolically inactive (Wightman and Fein, 2005).

2.2. Preparation of mineral powders

A high-defect kaolinite, KGa-2, from the Source Clay Repository, was used as the clay sorbent in our systems. Following a procedure similar to that used by Schroth and Sposito (1997), the kaolinite was washed repeatedly in a 1 M NaClO₄ solution that was previously adjusted to pH 3.0 with concentrated HCl. After each wash, the supernatant pH was measured, the clay suspension was centrifuged at 8100 g for 5 min to pellet the clay, and the supernatant was discarded. This process was repeated until the supernatant pH stabilized at 3.0. The clay was then washed in non-acidified solutions of NaClO₄, gradually decreasing in ionic strength from 1 M to 0.1 M. Three final washes in 0.1 M NaClO₄, the electrolyte and ionic strength of the adsorption experiments, were conducted, and the pH was stabilized at 4.5. The clay was then dried at 25 °C, ground to a fine powder, and stored in a sealed centrifuge tube.

HFO was produced by titrating a 1.0 l solution of 0.05 M Fe (NO₃)₃·9H₂O with small volumes of concentrated NaOH to increase the solution pH to 6.0. The solution was stirred for 24 h to allow the HFO to precipitate fully, after which the solution was decanted and the HFO powder was washed three times with 18 MΩ ultrapure water. The powder was dried at room temperature for 24 h and stored in a sealed polycarbonate test tube.

2.3. Cd adsorption experiments

Batch Cd adsorption experiments were performed under open atmosphere at initial Cd concentrations of 8.9×10^{-5} M and 8.9×10^{-6} M, referred to hereafter as '10 ppm' and '1 ppm' experiments for simplicity. To determine the stability constants for each important Cd–surface complex, we measured the adsorption of Cd onto each sorbent separately as a function of pH. 1 g l⁻¹ of kaolinite, *B. subtilis*, or HFO was suspended in a 0.1 M NaClO₄ solution. A small volume of a 1000 mg l⁻¹ Cd stock solution was added to each bacterial suspension, with the amount determined gravimetrically, to achieve the desired Cd concentration. The Cd stock solution was prepared from a Cd(ClO₄)₂ salt. While stirring, the bulk suspension then was divided into 8 ml aliquots in polycarbonate test tubes, and small volumes of concentrated HNO₃ or NaOH were used to adjust the pH of each experiment so that a set covered a pH range between approximately 2 and 8. This pH range was selected to avoid the precipitation of Cd-hydroxides that occurs at the experimental Cd concentrations under higher pH conditions. The test tubes were then placed on a rotary shaker for 2 h, after which the final pH of each solution was measured. Two hours is sufficient time for aqueous Cd to equilibrate with cell wall functional groups (e.g., Yee and Fein, 2001), and a short enough period of time to prevent cell lysis during the adsorption experiment. After pH was measured, the experimental systems were centrifuged at 8100 g for 10 min to pellet the solid sorbent, and the supernatant was decanted and filtered through 0.45 μm Nylon membranes. The resulting filtered supernatants were acidified with 15 μl of 15.8 N HNO₃.

All filtered experimental supernatants were analyzed for Cd concentrations on the same day that they were collected, using inductively coupled plasma-optical emission spectroscopy (ICP-OES).

The amount of Cd adsorbed in each experimental system was determined by difference between the initial known Cd concentration in each experiment and the measured Cd concentration remaining in solution after equilibration with each sorbent. Aqueous Cd standards for ICP-OES calibration were prepared gravimetrically from a 1000 mg l⁻¹ Cd stock solution made from a Cd(NO₃)₂ salt, diluted to desired concentrations using the same 0.1 M NaClO₄ matrix as was used in the experimental systems. The Cd signal strength reported by the ICP-OES did not vary significantly with solution ionic strength, and analytical uncertainty as determined by a repeat analysis of standards was ± 3%.

Parent suspensions, consisting of 1 g l⁻¹ of each sorbent in 0.1 M NaClO₄, were mixed to generate systems containing two or three sorbents. In this way, the total sorbent concentration in one-, two-, and three-component systems was a constant 1 g l⁻¹, while the ratio of one sorbent to another could be varied. After mixing, a small aliquot of the Cd stock solution described above was added to the mixture. The solutions were divided into polycarbonate test tubes and the pH adjusted with small volumes of concentrated NaOH or HNO₃. The test tubes were then placed on a rotary shaker for 2 h, after which the equilibrium pH was measured. Centrifugation, filtration, and acidification sampling procedures were the same as those described above for the one-component systems.

In the experiments that involved acetate, 1 g l⁻¹ of sorbent was initially suspended in a 0.1 M NaClO₄ solution that contained 0.3 M acetate as sodium acetate. The suspension was then spiked with Cd to the desired concentration, and the experiments were conducted using the same procedure as described above. Experiments in the presence of dissolved acetate were conducted with one-sorbent kaolinite, *B. subtilis*, or HFO systems, and in the presence of all three sorbents simultaneously.

3. Results and discussion

3.1. Cd adsorption onto individual sorbents

The extents of Cd adsorption onto 1 g l⁻¹ HFO, 1 g l⁻¹ *B. subtilis* cells, and 1 g l⁻¹ kaolinite are depicted as a function of pH for the 10 ppm (Fig. 1A) and 1 ppm Cd (Fig. 1B) experiments. For each of the sorbents, Cd adsorption generally increases with increasing pH from 2 to 8. At both Cd concentrations, HFO adsorbs less than 20% of the total Cd in the systems below pH 5, and the extent of adsorption increases most significantly between pH 6 and 7 to nearly 100% in the 1 ppm Cd experiments and to nearly 80% in the 10 ppm Cd experiments. *B. subtilis* cells exhibit a shallower pH adsorption edge than does the HFO. The cells adsorb Cd to a similar extent to that of HFO below pH 6, but at higher pH, the extent of adsorption does not increase as much for the bacterial systems as it does for HFO, with the maximum extent of adsorption being 75% at pH 7.9 for the 1 ppm Cd experiments, and 40% at pH 7.7 for the 10 ppm Cd experiments. The kaolinite clay adsorbs Cd more weakly on a per gram basis than the HFO or the *B. subtilis* cells, never exceeding 20% of the total Cd concentration in the experiments.

3.2. Modeling approach

We employ a non-electrostatic model (NEM) surface complexation approach to model the Cd adsorption behavior to *B. subtilis* cells and to kaolinite, and we use a diffuse double layer model (DLM) to describe Cd adsorption to the HFO surface. Fein et al. (2005) performed potentiometric titrations of *B. subtilis* cells and demonstrated that both electrostatic and non-electrostatic models can fit potentiometric titration data for bacteria equally well, but that surface electric field effects are small for bacteria. For our modeling, we employ the Fein et al. (2005) four-site NEM to describe the surface protonation and site concentrations on the bacterial cell wall. The

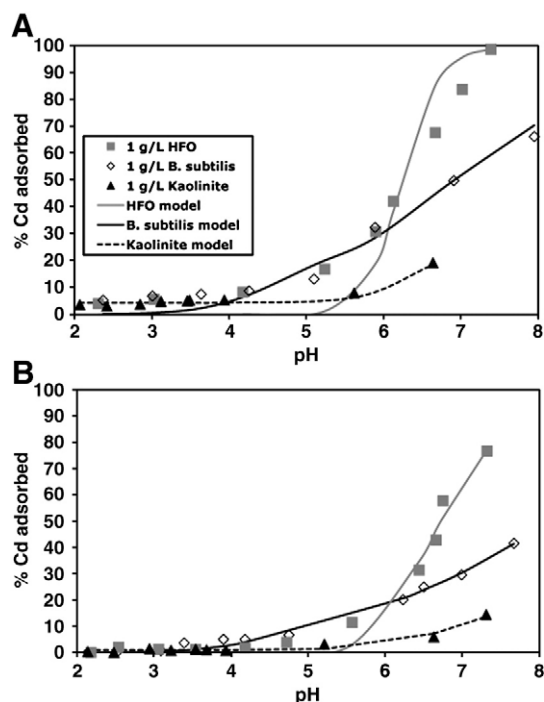


Fig. 1. Adsorption of (A) 8.9×10^{-5} M Cd(II) and (B) 8.9×10^{-6} M Cd(II) to 1 g l⁻¹ HFO (■), 1 g l⁻¹ *B. subtilis* cells (◇), and 1 g l⁻¹ kaolinite (▲). Curves represent best-fit models to HFO (grey curve), *B. subtilis* (solid curve), and kaolinite (dashed curve) Cd adsorption data.

NEM approach may be preferable for complex geologic applications because it requires fewer fitting parameters than do electrostatic models of surface electric field effects. Schroth and Sposito (1997, 1998) conducted potentiometric titrations and metal adsorption experiments on the KGa-2 kaolinite clay used here, and employed two amphoteric, proton-active surface sites and a permanent, pH independent structural charge site to describe protonation and metal adsorption onto the clay surface. The permanent structural charge sites account for the adsorption effects of isomorphous substitutions in the mineral lattice; the amphoteric sites likely represent surface silica and alumina functional groups. The surface reactivity of HFO is described by the DLM of Dzombak and Morel (1990) that employs strong and weak amphoteric surface sites to explain surface protonation and metal adsorption at ≡FeOH sites. The protonation and cadmium adsorption reactions, and related stability constants for each sorbent are listed in Table 1.

3.2.1. Calculation of Cd-*B. subtilis* stability constants

The basis of the Cd adsorption model is the non-electrostatic protonation model of Fein et al. (2005). In this model, deprotonation of cell wall organic acid functional groups is described by the generic reaction:



where A_i represents one of the four organic acid functional group types needed to account for the protonation behavior of the cell wall ($i = 1-4$), and R represents the cell wall macromolecule to which the functional group A_i is attached. The mass action equation for the deprotonation reaction is:

$$K_a = \frac{[R-A_i^-] a_{H^+}}{[R-A_i(H)^0]}, \quad (2)$$

where K_a is the acidity constant for Reaction (1), the brackets represent molar concentrations of the bacterial surface species, and a_{H^+} is the

Table 1
Proton and Cd reactions at *Bacillus subtilis* cell walls, kaolinite, and HFO.

<i>Bacillus subtilis</i> bacterial cells		
Reaction	[Site] ^a	pK _a ^b
R–A ₁ (H) ⁰ ↔ H ⁺ + R–A ₁ [–]	75	3.3
R–A ₂ (H) ⁰ ↔ H ⁺ + R–A ₂ [–]	96	4.7
R–A ₃ (H) ⁰ ↔ H ⁺ + R–A ₃ [–]	31	6.8
R–A ₄ (H) ⁰ ↔ H ⁺ + R–A ₄ [–]	75	8.9
	log K _{Cd, 1 ppm}	log K _{Cd, 10 ppm}
Cd ²⁺ + R–A ₂ [–] ↔ R–A ₂ (Cd) ⁺	3.4	3.3
Cd ²⁺ + R–A ₃ [–] ↔ R–A ₃ (Cd) ⁺	4.7	4.3
Cd ²⁺ + R–A ₄ [–] ↔ R–A ₄ (Cd) ⁺	4.8	4.9
Kaolinite KGa-2		
Reaction	[Site] ^a	log K ^c
XOH + H ⁺ ↔ XOH ₂ ⁺	35.9	3.5
XOH ↔ XO [–] + H ⁺		–7.2
YO [–]	13.6	
	log K _{Cd, 1 ppm}	log K _{Cd, 10 ppm}
XOH + Cd ²⁺ ↔ XO–Cd ⁺ + H ⁺	–2.8	–2.4
YO [–] + Cd ²⁺ ↔ YO–Cd ⁺	3.9	3.9
HFO		
Reaction	[Site] ^a	log K ^d
≡Fe ^s OH ⁰ + H ⁺ ↔ ≡FeOH ₂ ⁺	56	7.29
≡Fe ^s OH ⁰ ↔ ≡FeO [–] + H ⁺		–8.93
≡Fe ^w OH ⁰ + H ⁺ ↔ ≡FeOH ₂ ⁺	2247	7.29
≡Fe ^w OH ⁰ ↔ ≡FeO [–] + H ⁺		–8.93
	log K ^e _{Cd, 1 ppm}	log K ^e _{Cd, 10 ppm}
≡Fe ^s OH ⁰ + Cd ²⁺ ↔ ≡FeO–Cd ⁺ + H ⁺	0.42	–0.3
≡Fe ^w OH ⁰ + Cd ²⁺ ↔ ≡FeO–Cd ⁺ + H ⁺	N/A	–3.6

^aConcentration of sites, in μmol g^{–1}.

^bValues from Fein et al. (2005).

^cValues from Schroth and Sposito (1998).

^dValues from Dzombak and Morel (1990).

^elog K_{Cd} values for each sorbent are calculated from best-fit models to one-component Cd adsorption data collected in this study.

activity of aqueous protons in the bulk solution. The four protonation constant (pK_a) values used to describe proton binding onto the cell wall in the Fein et al. (2005) model are 3.3, 4.7, 6.8, and 8.9.

We describe Cd adsorption onto deprotonated functional groups on the bacterial surface according to:



The equilibrium constant (K_{i–Cd}) for complexation Reaction (3) involving Site *i* is defined by:

$$K_{i-\text{Cd}} = \frac{[\text{R}-\text{A}_i(\text{Cd})^+]}{[\text{R}-\text{A}_i^-] a_{\text{Cd}^{2+}}}, \quad (4)$$

where [R–A_i[–]] represents the concentration of deprotonated cell wall functional group A_i, [R–A_i(Cd)⁺] represents the concentration of cell wall functional group A_i that is complexed with Cd²⁺, and a_{Cd²⁺} is the activity of Cd²⁺ in solution after equilibrium is attained.

The objective of the Cd–bacteria experiments is to constrain values of K_{i–Cd} that can be used to model Cd–bacterial adsorption in the more complex systems. In systems with low metal:sorbent concentration ratios, Cd binding onto only one cell wall functional group is required to describe Cd adsorption (e.g., Fein et al., 1997; Yee and Fein, 2001; Fein et al., 2001). However, systems having higher metal:sorbent ratios may involve more than one Cd-binding site to obtain the best-fit (Yee and Fein, 2001; Borrok and Fein, 2004).

We use the computer program FITEQL 2.0 (Westall, 1982) to solve for the stability constants for all metal-sorbent surface complexes. This program accounts for the aqueous speciation of Cd, and all Cd–surface complexes. We include aqueous cation hydrolysis reactions, using the constants reported by Baes and Mesmer (1976; Table 2). We test a range of models that invoke Cd binding onto between one and four bacterial sites. The relative goodness-of-fit of each model is determined by comparing the overall variance parameter, V(Y), calculated by FITEQL. In both the 10 and 1 ppm bacteria-only systems (Fig. 1), a model involving Cd adsorption onto bacterial Sites 2, 3, and 4 yields the lowest V(Y) value. For the 10 ppm Cd experiments (Fig. 1A), the calculated stability constants log K_{2–Cd}, log K_{3–Cd}, and log K_{4–Cd} are 3.3, 4.3, and 4.9, respectively. The log stability constant values calculated using the 1 ppm Cd experimental data (Fig. 1B) are similar: 3.4, 4.7, and 4.8. Borrok et al. (2004) invoked Sites 2 and 3 to describe the adsorption of 10 ppm Cd onto 1 g l^{–1} of *B. subtilis*, yielding similar calculated values for log K_{2–Cd} and log K_{3–Cd} of 3.4 and 4.6, respectively, despite the different Cd:bacterial site ratio of their experiments. We use the equilibrium constants calculated for each sorbate at 1 ppm and 10 ppm initial Cd concentrations to describe Cd adsorption to *B. subtilis* in systems containing two- and three-sorbent mixtures.

3.2.2. Kaolinite proton and metal adsorption model

Schroth and Sposito (1997, 1998) described the surface charge properties of KGa-2, and developed a NEM to describe proton and metal adsorption to the surface of the kaolinite. This model accounts for proton activity with a single amphoteric surface site, XOH, according to the reactions:



The log equilibrium constant values for Reactions (5) and (6) are 3.5 and –7.2, respectively (Schroth and Sposito, 1998). In this approach, Cd adsorption is described by complexation both with the amphoteric site and an additional permanent negatively charged surface site, YO[–], according to:



We use values for the equilibrium constants for Reactions (5) and (6) and for site concentrations from Schroth and Sposito (1998), and we use the measured Cd adsorption behavior of kaolinite as a function of pH to solve for the equilibrium constants for Reactions (7) and (8). We calculate log K₇ and log K₈ values of –2.8 and 3.9 from the 10 ppm Cd adsorption data, and –2.4 and 3.9 from the 1 ppm Cd experimental data, respectively. The best-fit model for the 10 ppm data is depicted in Fig. 1A, and that for the 1 ppm data in Fig. 1B. Our 10 ppm data sets can be adequately described by Cd adsorption at the XOH site only (Eq. (7)), where a low percentage of free Cd is adsorbed

Table 2
Cadmium hydrolysis reactions.

Reaction	log K ^a
Cd ²⁺ + H ₂ O ↔ CdOH ⁺ + H ⁺	–10.08
Cd ²⁺ + 2H ₂ O ↔ Cd(OH) ₂ ⁰ + 2H ⁺	–20.35
Cd ²⁺ + 3H ₂ O ↔ Cd(OH) ₃ [–] + 3H ⁺	–33.3
Cd ²⁺ + 4H ₂ O ↔ Cd(OH) ₄ ^{2–} + 4H ⁺	–47.35
2Cd ²⁺ + H ₂ O ↔ Cd ₂ OH ³⁺ + H ⁺	–9.39
4Cd ²⁺ + 4H ₂ O ↔ Cd ₄ (OH) ₄ ⁴⁺ + 4H ⁺	–32.85

^a Values from Baes and Mesmer (1976).

below pH 5. However, it is necessary to invoke the YO⁻ site to describe the significant adsorption observed below pH 5 in 1 ppm experiments. The best-fit, as quantified by the V(Y) parameter, is achieved when both XOH and YO⁻ sites are invoked for both the 10 ppm and 1 ppm data sets, so both models utilize these two sites.

Schroth and Sposito (1998) calculated log K₇ and log K₈ values of -1.45 and 3.65, respectively. Our equilibrium constant values, particularly that of K₇, are significantly different. Were we to use the log K₇ value given by Schroth and Sposito (1998) to model our 10 ppm and 1 ppm data, the models would predict significantly more Cd adsorption than we observe below pH 5, where the structural YO⁻ site dominates adsorption. For example, in the 10 ppm experiments we never observe more than 15% of the Cd adsorbed to the kaolinite surface at any pH. Using the Schroth and Sposito (1998) constants to model our data yields predictions of more than 30% adsorption between pH 5 and 7. Schroth and Sposito (1998) conducted their experiments with 10 g l⁻¹ kaolinite and 8.9 × 10⁻⁷ M Cd (0.1 ppm), and observed a range of 30% to 90% Cd removal from solution across the pH range 2 to 8. Our systems contain 10 or 100 times the initial Cd concentration, and only 1 g l⁻¹ kaolinite. Because their data describe a greater range of adsorption behavior, the equilibrium constants calculated by Schroth and Sposito (1998) are likely applicable to a wider range of conditions than ours. Differences in the calculated log K₇ value could be attributed to differences in equilibration time between our study and that of Schroth and Sposito (1998), differences in electrolyte ionic strength, or the large difference in Cd:kaolinite ratios. However, because the other adsorption measurements in our study are conducted under the same conditions as these, and the constants are reasonably similar, we use our Cd-kaolinite stability constants calculated from 1 ppm and 10 ppm adsorption data (Table 1) in the multi-sorbent predictive models of the same Cd concentrations.

3.2.3. HFO proton and metal adsorption model

Dzombak and Morel (1990) described the reactive sites on the surface of HFO using two types of amphoteric sites with the same acidity constants, but with different site concentrations. The strong site, ≡Fe^sOH, represents a subset of low concentration sites with a high affinity to adsorb metal cations. The weak site, ≡Fe^wOH, is a high concentration site with lower cation affinity, useful for describing cation adsorption behavior in systems with higher sorbate:sorbent ratios. Both sites react with protons according to:

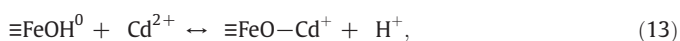


The mass action equations in the DLM include the Boltzmann factor, $\exp\left(-\frac{\Delta z \psi F}{RT_k}\right)$, to account for the electrostatic effects on surface free energies (Bethke, 2007), where Δz is the change in surface charge due to cation adsorption, ψ is the surface potential, F is Faraday's constant, R is the ideal gas constant, and T_k is the temperature, in Kelvin. Incorporating this factor into the mass law equations for the reactions in Eqs. (9) and (10) yields:

$$K_{11} \cdot e^{\left(-\frac{\psi F}{RT_k}\right)} = \frac{[\equiv\text{FeOH}_2^+]}{[\equiv\text{FeOH}^0] a_{\text{H}^+}} \quad (11)$$

$$K_{12} \cdot e^{\left(-\frac{\psi F}{RT_k}\right)} = \frac{[\equiv\text{FeO}^-] a_{\text{H}^+}}{[\equiv\text{FeOH}^0]} \quad (12)$$

log K₁₁ and log K₁₂ values are given as 7.29 and -8.93, respectively (Dzombak and Morel, 1990). Adsorption of aqueous Cd²⁺ onto both the strong and weak HFO surface sites can be represented as:



and the equilibrium constant, K_{HFO-Cd}, is described by:

$$K_{\text{HFO}-\text{Cd}} \cdot e^{\left(-\frac{\psi F}{RT_k}\right)} = \frac{[\equiv\text{FeOH}^0] a_{\text{Cd}^{2+}}}{[\equiv\text{FeO}-\text{Cd}^+] a_{\text{H}^+}} \quad (14)$$

At low sorbate:sorbent concentrations, where there are abundant surface sites available, metal adsorption can be described by adsorption to the strong site, ≡Fe^sOH, only. By modeling 24 sets of pH-dependent Cd adsorption data, Dzombak and Morel (1990) calculated an average stability constant, log K_{HFO-Cd}, of 0.47 for the strong site. Using one set of pH-dependent adsorption data in which the sorbate:sorbent ratio is high, they calculated a log K_{HFO-Cd} value of -2.90 for the weak site. In this same data set, Dzombak and Morel (1990) calculated the log K_{HFO-Cd} of the strong adsorption site to be -0.51, significantly below the value of 0.47 calculated from the low sorbate:sorbent ratio data. Our 10 ppm Cd experiments have a high sorbate:sorbent ratio, and it is necessary to invoke binding onto both the strong and the weak sites to fit our data. For these data, we calculate values for the strong and weak sites to be -0.3 and -3.6, respectively. To describe adsorption of 1 ppm Cd to 1 g l⁻¹ HFO, a lower sorbate:sorbent ratio, it is only necessary to invoke the strong site, consistent with similar datasets in Dzombak and Morel (1990). The log K_{HFO-Cd} value that we calculate for the strong site from the 1 ppm Cd data is 0.42. The best-fit to the 10 ppm Cd experiments closely match the observed adsorption behavior (Fig. 1A). However, the best-fit model of the 1 ppm Cd data exhibits a steeper adsorption edge than is observed in the experimental data, so that the model fails to account for significant adsorption observed below pH 5.5. Several best-fit models to sets of Cd adsorption data in Dzombak and Morel (1990) exhibit a similar trend. To account for Cd adsorption at lower pH, a model would need to incorporate a site that deprotonates at lower pH.

3.3. Cd adsorption to two-component mixtures

Figs. 2, 3, and 4 compare the measured extents of Cd adsorption onto 2-component sorbent mixtures to the CA model predictions of the Cd adsorption behaviors. The graphs also depict the same model fits to the one-component end-member systems that are shown in Fig. 1 for reference. Models of the two-sorbent mixtures use the acidity and equilibrium constants calculated in the SCMs described in Section 3.2 and compiled in Table 1 to independently predict the extent of Cd adsorption in each two-sorbent system. Molal ratios of site concentrations for each mixture are listed in Table 3.

The Cd adsorption behaviors for mixtures of HFO and *B. subtilis* cells are depicted in Fig. 2. Experiments containing 75% HFO and 25% *B. subtilis* (by mass) exhibit Cd adsorption behavior similar to that of the corresponding 100% HFO systems. In this system, *B. subtilis* cells contribute 54% of the potential Cd adsorption sites on a molal basis, and HFO the remaining 46%. Clearly, Cd preferably binds to the HFO surface relative to the sites on the *B. subtilis* cell walls. Mixtures of 25% HFO and 75% *B. subtilis* adsorb significantly less Cd than the 100% HFO experiments, but more than was observed in systems containing 100% *B. subtilis* cells. HFO has significantly lower site concentrations compared to *B. subtilis*, contributing less than 46% of the surface sites when it is 75% of the mass of the mixture, and approximately 8% of the sites when it is 25% of the mixture by mass. The predictive models (solid curves) describe the 10 ppm data reasonably well, but exhibit similar misfits to the 1 ppm data to those observed between the model and the 100% HFO data. Lund et al. (2008) observed that discrepancies in fitting metal adsorption to the pure phases caused discrepancies in the predicted fits of multi-component systems using the CA approach, and we observe the same phenomenon. Thus, the difference between the model predictions

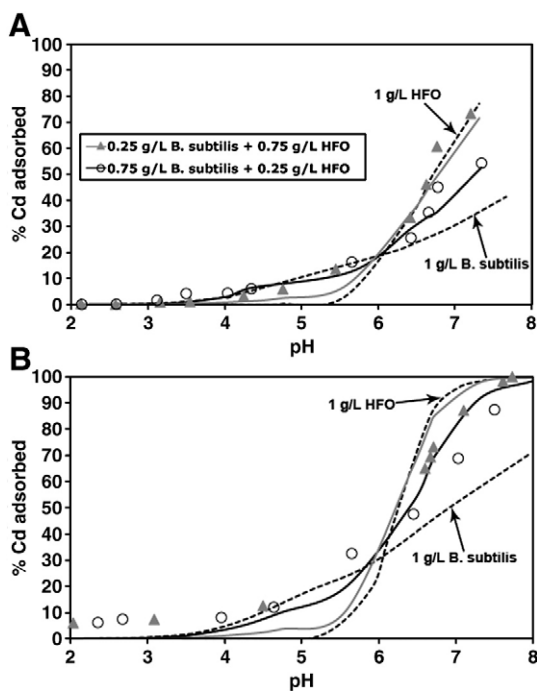


Fig. 2. Adsorption of (A) 8.9×10^{-5} M Cd(II) and (B) 8.9×10^{-6} M Cd(II) to mixtures of HFO and *B. subtilis* cells. Symbols and solid curves represent adsorption data and predicted adsorption behavior for two-sorbent mixtures, respectively, including 0.75 g l^{-1} HFO + 0.25 g l^{-1} *B. subtilis* cells (\blacktriangle , grey curve), and 0.25 g l^{-1} HFO + 0.75 g l^{-1} *B. subtilis* cells (\circ , black curve). Dashed curves represent best-fit models to 1 g l^{-1} HFO and *B. subtilis* end members from Fig. 1.

and experimental data in the two-component 1 ppm experiments is likely caused by the relatively poor fit of the one-component 1 ppm Cd + HFO model.

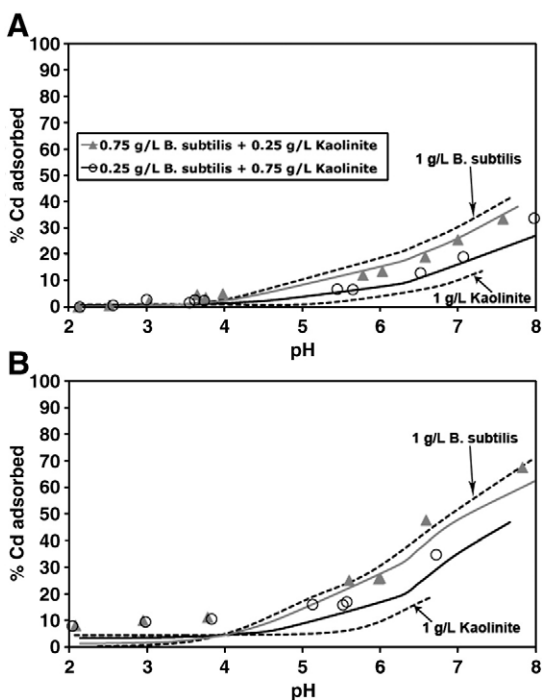


Fig. 3. Adsorption of (A) 8.9×10^{-5} M Cd(II) and (B) 8.9×10^{-6} M Cd(II) to mixtures of kaolinite and *B. subtilis* cells. Symbols and solid curves represent adsorption data and predicted adsorption for two-sorbent mixtures, respectively, including 0.75 g l^{-1} *B. subtilis* cells + 0.25 g l^{-1} kaolinite (\blacktriangle , grey curve), and 0.25 g l^{-1} *B. subtilis* cells + 0.25 g l^{-1} kaolinite (\circ , black curve). Dashed curves represent best-fit models to 1 g l^{-1} kaolinite and *B. subtilis* end members from Fig. 1.

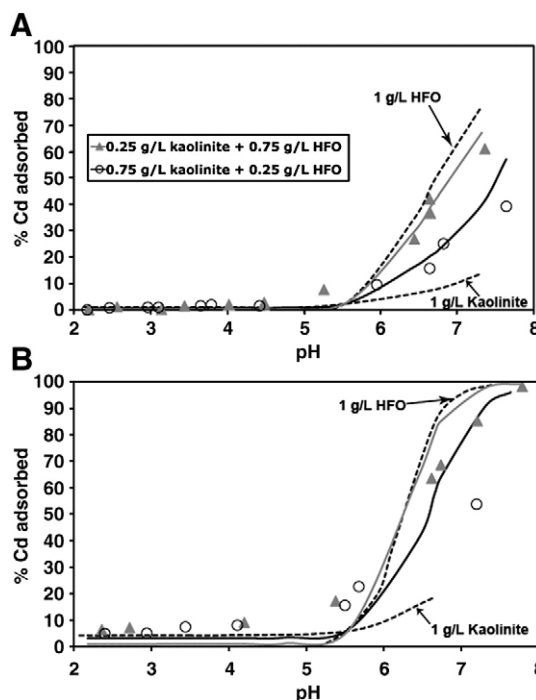


Fig. 4. Adsorption of (A) 8.9×10^{-5} M Cd(II) and (B) 8.9×10^{-6} M Cd(II) to mixtures of HFO and kaolinite. Symbols and solid curves represent adsorption data and predicted adsorption for two-sorbent mixtures, respectively, including 0.75 g l^{-1} HFO + 0.25 g l^{-1} kaolinite (\blacktriangle , grey curve), and 0.25 g l^{-1} HFO + 0.75 g l^{-1} kaolinite (\circ , black curve). Dashed curves represent best-fit models to 1 g l^{-1} HFO and kaolinite end members from Fig. 1.

Fig. 3 illustrates Cd adsorption behavior onto mixtures of *B. subtilis* and kaolinite. These data show Cd adsorption decreasing systematically with increasing kaolinite in the mixture; 100% *B. subtilis* adsorbs the greatest portion of free Cd, followed by the 75% *B. subtilis* + 25% kaolinite mixture, the 25% *B. subtilis* + 75% kaolinite mixture, and the 100% kaolinite adsorption experiments. In experiments containing 75% *B. subtilis* and 25% kaolinite by mass, the bacteria represent more than 92% of the surface sites on a molal basis, and in mixtures of 25% *B. subtilis* and 75% kaolinite by mass, *B. subtilis* contribute nearly 58% of the reactive sites. However, the majority of Cd adsorption below pH 4 is predicted to occur onto the permanent structural site, YO^- , of kaolinite. In both the 10 ppm and 1 ppm Cd experiments, the predictive models provide reasonable fits to the measured extents of adsorption in the *B. subtilis*–kaolinite systems.

Cd adsorption onto mixtures of HFO and kaolinite is depicted in Fig. 4. A mixture of 75% HFO + 25% kaolinite adsorbs free Cd to a similar extent as the 100% HFO experiments, with only slightly less

Table 3
Molal site concentrations of sorbents in two- and three-component mixtures.

Mixture ^a	HFO ^b	<i>B. subtilis</i> ^b	Kaolinite ^b
75% HFO + 25% <i>B. subtilis</i>	42.2	50.5	
25% HFO + 75% <i>B. subtilis</i>	14.0	151.5	
75% HFO + 25% kaolinite	42.2		12.4
25% HFO + 75% kaolinite	14.0		37.1
75% <i>B. subtilis</i> + 25% kaolinite		151.5	12.4
25% <i>B. subtilis</i> + 75% kaolinite		50.5	37.1
80% HFO + 10% <i>B. subtilis</i> + 10% kaolinite	45.0	20.2	5.0
10% HFO + 80% <i>B. subtilis</i> + 10% kaolinite	5.6	161.6	5.0
10% HFO + 10% <i>B. subtilis</i> + 80% kaolinite	5.6	20.2	39.6
33% HFO + 33% <i>B. subtilis</i> + 33% kaolinite	18.7	67.3	16.5

^a All mixtures add to 1 g l^{-1} sorbent.

^b Site concentrations given in $\mu\text{mol g}^{-1}$.

adsorption above pH 7. The 25% HFO + 75% kaolinite mixture adsorbs substantially more Cd than experiments conducted with 100% kaolinite, but less than those with 100% HFO. These results suggest that HFO dominates the adsorption behavior of Cd in experiments where it is 75% of the total sorbent mass, and strongly influences Cd adsorption even as a minor component of 25% of the sorbent mass. HFO has nearly identical site concentrations as kaolinite, contributing approximately 77% of the surface sites when it is 75% of the mixture, and 27% of the sites when it is 25% of the mixture. The HFO-like adsorption behavior of both mixtures attests to the higher affinity of HFO for adsorption of Cd compared to that of kaolinite and *B. subtilis*. Predictive models of the mixtures containing 10 ppm Cd fit the experimental data well, but the models deviate from the 1 ppm data significantly. This difference can be attributed again to the poor fit of the one-component 1 ppm Cd + HFO model.

Dissolved acetate, CH_3COO^- , is used to determine the effect of aqueous metal-organic complexation on the adsorption of Cd to one- and three-sorbent systems. We conduct these experiments with 1 g l^{-1} sorbent in the presence of 0.3 M acetate, as sodium acetate. To predict the effects of aqueous Cd-acetate complexation on the Cd adsorption

behavior in one-component systems with acetate, we use the stability constants for the Cd-sorbent complexes that we calculated from our one-component Cd adsorption experiments, along with the acetate acidity constant and Cd-acetate stability constants for the 1:1, 1:2, 1:3, and 1:4 Cd:acetate complexes from the literature (Martell and Smith, 1977). Fig. 5 compares the measured extents of Cd adsorption in the absence of acetate (solid squares) and in the presence of acetate (open circles). HFO experiments and models at 10 ppm and 1 ppm are depicted in Fig. 5A and B, respectively. The predictive models that include Cd-acetate complexation (dashed curves) dramatically underestimate the extent of adsorption observed in the experiments at all pH values between 2 and 8. The misfit at low pH, between 2 and 5.5, is less severe than the misfit of the high pH data, and likely stems from the failure of the basic HFO model to account for Cd adsorption at low pH. Shen et al. (2001) described the adsorption of Pb to soil in an acetate-bearing system by proposing that the aqueous Pb-acetate complex, $\text{Pb}(\text{CH}_3\text{COO})^+$, adsorbs to surface sites as a ternary site-Pb-acetate complex. Similarly, in our systems the 1:1 Cd-acetate complex, $\text{Cd}(\text{CH}_3\text{COO})^+$, dominates the aqueous Cd speciation. To account for the observed adsorption behavior, we invoke ternary site-Cd-acetate complexation to account for the discrepancy between

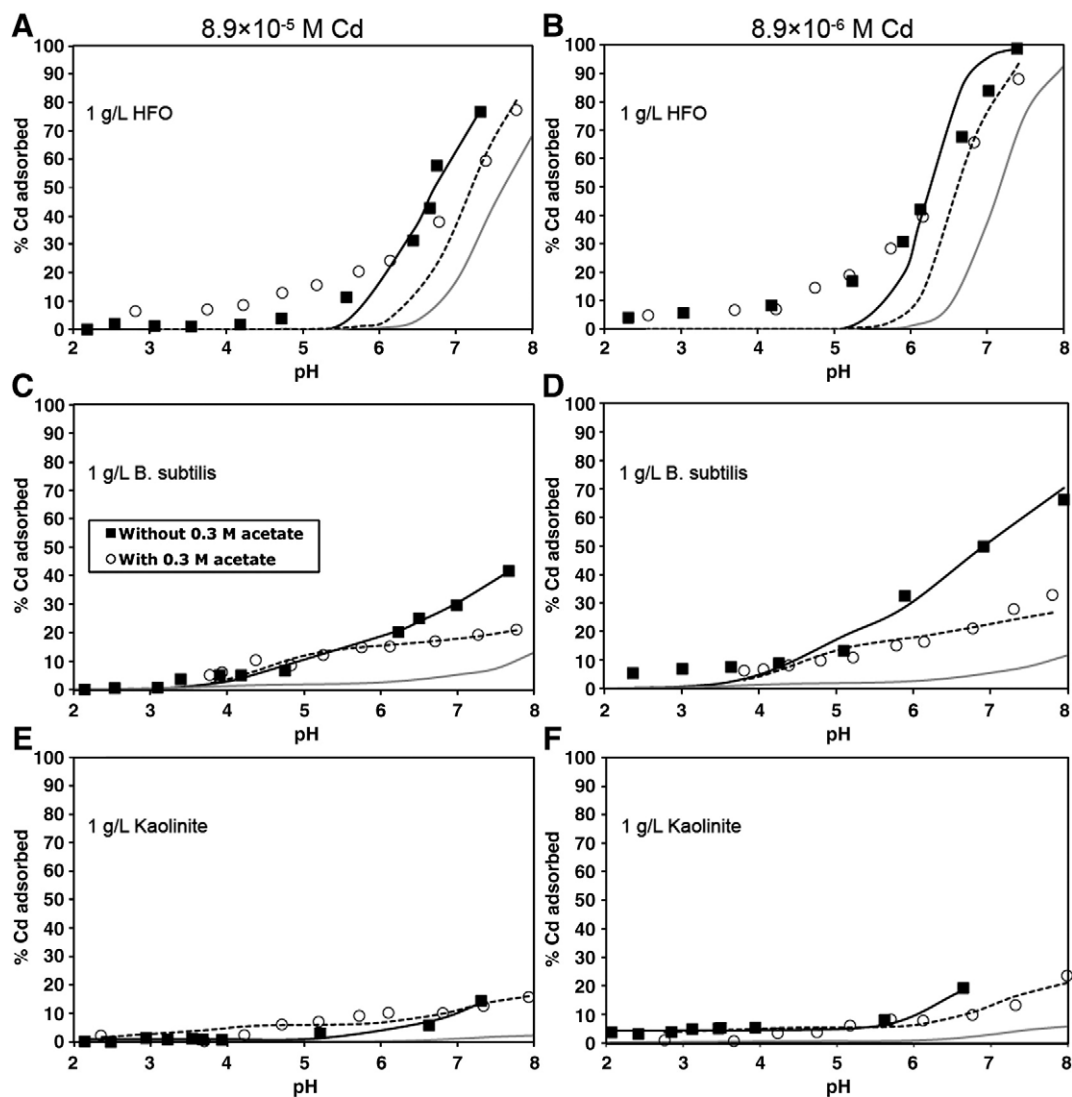
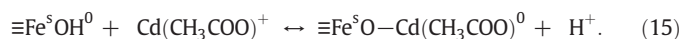


Fig. 5. Adsorption of 8.9×10^{-5} M Cd to 1 g l^{-1} A) HFO, C) *B. subtilis*, and E) kaolinite, and 8.9×10^{-6} M Cd to B) HFO, D) *B. subtilis*, and F) kaolinite. Filled symbols and solid curves represent adsorption data and predicted adsorption for mixtures without acetate, respectively. Open symbols represent adsorption data in the presence of 0.3 M acetate. The grey curve indicates the predicted extent of adsorption in acetate experiments without the adsorption of a Cd-acetate complex, and the dashed curve is the best-fit model including a Cd-acetate ternary surface complex.

the predicted extents of adsorption and the higher extents that were observed, according to:



The equilibrium constant, K_{15} , for the surface–Cd–acetate ternary complex is calculated using the previously-determined Cd–surface constants, and solving for the best-fit ternary surface complex constant. The calculated $\log K_{15}$ value from this approach is 0.9. The grey curves in Fig. 5A and B represent these best-fit models. Adsorption of the Cd–acetate complex improves the fits substantially at high pH, but the models continue to underpredict Cd adsorption below pH 7. This is likely due to the relatively poor fit of the one-component HFO model, and potentially because there are other ternary interactions that must be considered to model the data accurately. Our models suggest that in systems containing HFO and an organic ligand, the CA approach may not be sufficient to describe Cd adsorption behavior unless ternary interactions between important aqueous complexes and the HFO surface are considered.

Fig. 5C and D depict the adsorption of 10 ppm and 1 ppm Cd to *B. subtilis* cells, respectively. The model predictions of Cd adsorption in the presence of acetate (dashed curves) underestimate the actual extent of adsorption (open circles) across the entire pH range studied here. This result suggests that an aqueous Cd–acetate complex may be adsorbing to the bacterial surface. Models invoking a complexation reaction between the $\text{Cd}(\text{CH}_3\text{COO})^+$ complex and either Site 2, 3, or 4 yield a better fit to the experimental data, but inclusion of this reaction at Site 2 only (Table 4) yields the best-fit (grey curve). Models invoking $\text{Cd}(\text{CH}_3\text{COO})^+$ adsorption at Sites 2 and 3, or Sites 2, 3, and 4 give fits that are equivalent to the Site 2-only model. We use the model invoking only Site 2 for its simplicity.

The adsorption of 10 ppm and 1 ppm Cd in the presence of kaolinite and acetate is displayed in Fig. 5E and F, respectively. As with the HFO and *B. subtilis*, the predictive model that does not invoke a ternary complex under-predicts the extent of Cd adsorption across the entire pH range. Poor, but improved fits are obtained when the aqueous $\text{Cd}(\text{CH}_3\text{COO})^+$ ligand is complexed with either the amphoteric (XOH) or permanent structural (YO^-) sites. The model invoking only the XOH site underestimates adsorption below pH 5, and one invoking only the YO^- site underestimates adsorption where pH is greater than 5. The best-fit (grey curve) is obtained when $\text{Cd}(\text{CH}_3\text{COO})^+$ adsorbs onto both sites simultaneously (Table 4). In the cases of the kaolinite and *B. subtilis* cells, the adsorption of the $\text{Cd}(\text{CH}_3\text{COO})^+$ complex from solution is sufficient to describe the observed data. Additionally, the stability constants of ternary surface–Cd–acetate complexes calculated for an individual sorbent are similar whether modeling adsorption data from the 1 ppm or 10 ppm experiments (see Table 4). For instance, the $\log K$ values for $\text{Cd}(\text{CH}_3\text{COO})^+$ complexation at Site 2 of the *B. subtilis* cells is calculated to be 4.81 from the 1 ppm data, and

4.83 from the 10 ppm data. This provides further evidence that the Cd ($\text{CH}_3\text{COO})^+$ complex is adsorbing to each sorbent, that we are using the correct ternary complexation stoichiometries (Table 4), and that these reactions are capable of accounting for adsorption over a range of Cd concentrations.

3.4. Cd adsorption to three-component mixtures

The adsorption behavior of 1 ppm Cd to three-component mixtures of HFO, *B. subtilis*, and kaolinite is illustrated in Fig. 6. Four mixtures of the sorbents are investigated, one where each component comprises 33% of the 1 g l^{-1} sorbent present (Fig. 6D), and three sets in which one of the sorbents is 80% of the total mass, and the remaining 2 sorbents represent 10% of the total mass, each. In the mixture where each component contributes 33% of the sorbent mass, the *B. subtilis* cells, HFO, and kaolinite contribute 66%, 18%, and 16% of the reactive sites, respectively. However, as in the two-component experiments containing HFO that are described in Section 3.3, the most Cd adsorption is observed in experiments that contain a greater fraction of HFO. The mixture of 80% HFO + 10% *B. subtilis* cells + 10% kaolinite (Fig. 6A) adsorbs Cd to a nearly identical extent as the 100% HFO system (see Fig. 1B). Mixtures containing only 10% HFO and 80% *B. subtilis* or kaolinite (Fig. 6B and C, respectively) adsorb Cd to a lesser extent. The lowest extent of Cd adsorption is observed in the single component kaolinite systems (Fig. 1). Thus, the Cd adsorption behavior in the ternary mixtures of these sorbents is directly related to the extent of adsorption observed in the single sorbent systems. All 3-component predictive models describe the adsorption data reasonably well. The predicted extent of adsorption in the system containing 80% HFO (Fig. 6A) shows minor discrepancies due to the fit of the pure HFO end-member. However, in mixtures of HFO, *B. subtilis* cells, and kaolinite, the CA approach is generally successful in predicting Cd adsorption at our experimental conditions.

The results of adsorption experiments conducted with three sorbents in the presence of 0.3 M acetate are depicted in Fig. 6 (open circles). The dashed curves represent the best-fit Cd adsorption models, including the ternary complexation reactions calculated in this study and listed in Table 4. Fig. 6A depicts Cd adsorption for a mixture of 0.8 g l^{-1} HFO + 0.1 g l^{-1} *B. subtilis* cells + 0.1 g l^{-1} kaolinite in the presence of acetate. Compared to the same mixture in the absence of acetate (solid squares), more adsorption is observed below pH 5, and less above pH 6. Similar trends with pH are observed in the other three-component mixtures, including: 0.1 g l^{-1} HFO + 0.8 g l^{-1} *B. subtilis* cells + 0.1 g l^{-1} kaolinite (Fig. 6B), 0.1 g l^{-1} HFO + 0.1 g l^{-1} *B. subtilis* cells + 0.8 g l^{-1} kaolinite (Fig. 6C), and 0.33 g l^{-1} HFO + 0.33 g l^{-1} *B. subtilis* cells + 0.33 g l^{-1} kaolinite (Fig. 6D). The predictive models of these ternary systems may underestimate Cd adsorption below pH 5 (Fig. 6) because of poor fit of the basis 1 ppm + HFO data (Fig. 1B) is carried into these models. At pH greater than 6, all one-sorbent models of HFO, kaolinite, or *B. subtilis* cells in the presence of acetate (Fig. 5B, D, and F, respectively) fit the experimental data well. The predictive models of three-sorbent systems with acetate may overestimate adsorption at higher pH due to particle adhesion which causes a decrease in Cd adsorption as reactive sites are blocked. In particular, HFO, which has positively-charged sites under all experimental conditions, may aggregate with negatively charged kaolinite particles and/or *B. subtilis* cells.

4. Conclusions

In this study, we test if the CA approach can account for Cd adsorption to mixtures including *B. subtilis* cells, HFO, kaolinite, and dissolved acetate. We first conduct Cd adsorption experiments onto each sorbent separately at two metal concentrations. Using acidity constants and site concentrations for each sorbent from the literature, we model these adsorption data to calculate Cd stability constants for

Table 4
Ternary complexation reactions.

	log K values ^a	
	1 ppm	10 ppm
HFO		
$\equiv\text{Fe}^{\text{S}}\text{OH}^0 + \text{Cd}(\text{CH}_3\text{COO})^+ \leftrightarrow \equiv\text{Fe}^{\text{S}}\text{O}-\text{Cd}-\text{CH}_3\text{CO}_2^0 + \text{H}^+$	0.87	0.79
$\equiv\text{Fe}^{\text{W}}\text{OH}^0 + \text{Cd}(\text{CH}_3\text{COO})^+ \leftrightarrow \equiv\text{Fe}^{\text{W}}\text{O}-\text{Cd}-\text{CH}_3\text{CO}_2^0 + \text{H}^+$	N/A	-2.89
<i>B. subtilis</i> cells		
$R-A_2^- + \text{Cd}(\text{CH}_3\text{COO})^+ \leftrightarrow R-A_2-\text{Cd}-\text{CH}_3\text{CO}_2^0$	4.81	4.83
Kaolinite		
$\text{XOH} + \text{Cd}(\text{CH}_3\text{COO})^+ \leftrightarrow \text{XO}-\text{Cd}-\text{CH}_3\text{CO}_2^0 + \text{H}^+$	-1.27	-1.32
$\text{YO}^- + \text{Cd}(\text{CH}_3\text{COO})^+ \leftrightarrow \text{YO}-\text{Cd}-\text{CH}_3\text{CO}_2^0$	5.75	6.03

^a log K values for each reaction are calculated from best-fit models of 1 ppm and 10 ppm Cd adsorption data.

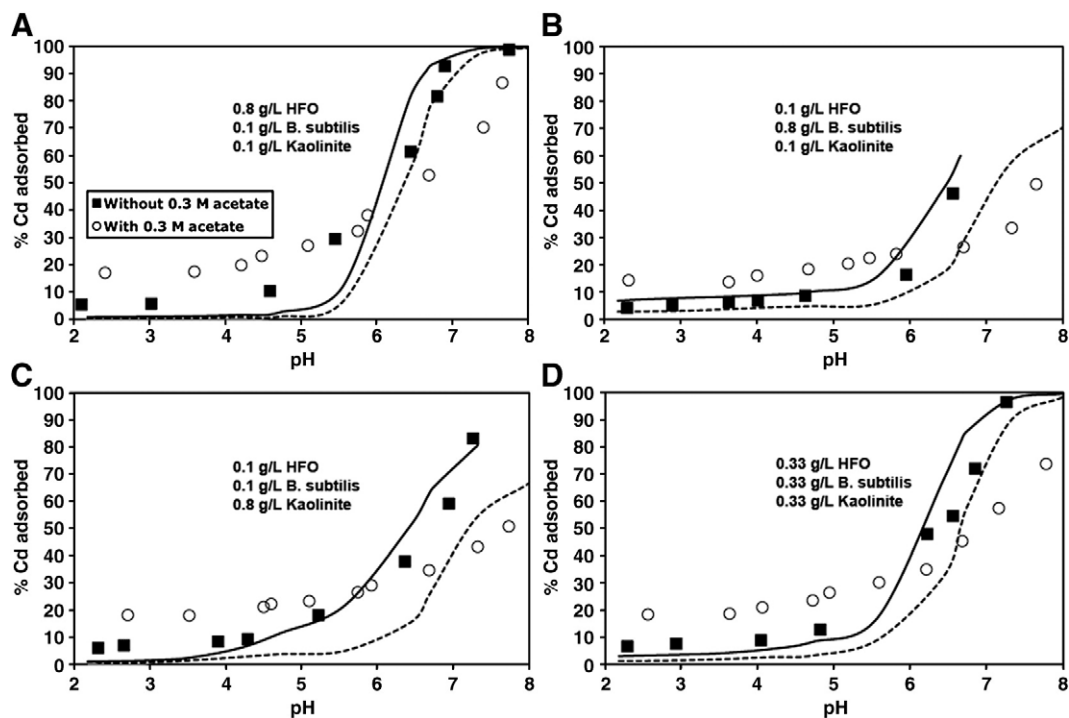


Fig. 6. Adsorption of 8.9×10^{-6} M Cd to three-component mixtures of HFO, kaolinite, and *B. subtilis*, and in the presence of 0.3 M dissolved acetate, respectively. Filled symbols and solid curves represent adsorption data and predicted adsorption for mixtures without acetate. Open symbols and dashed curves represent adsorption data and predicted adsorption in the presence of 0.3 M acetate, respectively. Sorbent mixtures include A) 0.8 g l^{-1} HFO + 0.1 g l^{-1} *B. subtilis* + 0.1 g l^{-1} kaolinite, B) 0.1 g l^{-1} HFO + 0.8 g l^{-1} *B. subtilis* + 0.1 g l^{-1} kaolinite, C) 0.1 g l^{-1} HFO + 0.1 g l^{-1} *B. subtilis* + 0.8 g l^{-1} kaolinite, D) 0.33 g l^{-1} HFO + 0.33 g l^{-1} *B. subtilis* + 0.33 g l^{-1} kaolinite.

each sorbent. Using these constants, we predict the extent of Cd adsorption in two- and three-component mixtures of the sorbents at various mass ratios. In the absence of dissolved acetate, the predictive models match experimental data well. However, in the systems that we test that contain dissolved acetate, the models predict a bigger decrease in adsorption than we observed. We account for this enhanced adsorption in the presence of acetate by invoking the adsorption of the $\text{Cd}(\text{CH}_3\text{COO})^+$ aqueous complex to each sorbent to form a ternary surface–Cd–acetate complex.

The component additivity approach represents a powerful means to extrapolate our understanding of metal adsorption in simple one-sorbent systems to predict metal distributions in complex multi-sorbent settings. Our results indicate that the CA approach is reasonably accurate under some circumstances. However, caution should be used when applying this approach to geologic systems, as site blockage and the formation of ternary complexes can significantly affect the accuracy of the CA predictions.

Acknowledgements

This research was supported by the National Science Foundation through an Environmental Molecular Science Institute grant to University of Notre Dame (EAR0221966), and by a University of Notre Dame Presidential Doctoral fellowship to D.S.A., sponsored by the Arthur J. Schmitt Foundation. We thank Jennifer Szymanski for assistance with many of the experiments reported here. A journal review by Carla Koretsky significantly improved the clarity and presentation of this study.

References

- Ali, M.A., Dzombak, D.A., 1996. Effects of simple organic acids on sorption of Cu^{2+} and Ca^{2+} on goethite. *Geochim. Cosmochim. Acta* 60, 291–304.
- Ams, D.A., Fein, J.B., Dong, H., Maurice, P.A., 2004. Experimental measurements of the adsorption of *Bacillus subtilis* and *Pseudomonas mendocina* onto Fe-oxyhydroxide-coated and uncoated quartz grains. *Geomicrobiol. J.* 21, 511–519.
- Baies Jr., C.F., Mesmer, R.E., 1976. *The Hydrolysis of Cations*. Wiley, New York. 489 p.
- Bethke, C.M., 2007. *Geochemical and Biogeochemical Modeling*. Cambridge University Press, New York. 543 p.
- Bethke, C.M., Brady, P.V., 2000. How the K-d approach undermines ground water cleanup. *Ground Water* 38, 435–443.
- Beveridge, T.J., 1989. Role of cellular design in bacterial metal accumulation and mineralization. *Annu. Rev. Microbiol.* 43, 147–171.
- Borrok, D., Fein, J.B., 2004. Distribution of protons and Cd between bacterial surfaces and dissolved humic substances determined through chemical equilibrium modeling. *Geochim. Cosmochim. Acta* 68, 3043–3052.
- Borrok, D., Fein, J.B., Tischler, M., O'Loughlin, E., Meyer, H., Liss, M., Kemner, K.M., 2004. The effect of acidic solutions and growth conditions on the adsorptive properties of bacterial surfaces. *Chem. Geol.* 209, 107–119.
- Buerge-Weirich, D., Behra, P., Sigg, L., 2003. Adsorption of copper, nickel, and cadmium on goethite in the presence of organic ligands. *Aquat. Geochem.* 9, 65–85.
- Covelo, E.F., Vega, F.A., Andrade, M.L., 2007. Competitive sorption and desorption of heavy metals by individual soil components. *J. Hazard. Mater.* 140, 308–315.
- Davis, J.A., Coston, J.A., Kent, D.B., Fuller, C.C., 1998. Application of the surface complexation concept to complex mineral assemblages. *Environ. Sci. Technol.* 32, 2820–2828.
- Dzombak, D.A., Morel, F.M.M., 1990. *Surface Complexation Modeling: Hydrated Ferric Oxide*. Wiley-Interscience, New York. 393pp.
- Fein, J.B., 2002. The effects of ternary surface complexes on the adsorption of metal cations and organic acids onto mineral surfaces. In: Hellmann, R., Wood, S.A. (Eds.), *Water–Rock Interactions, Ore Deposits, and Environmental Geochemistry: A Tribute to David A. Crerar*. Geochemical Society, Special Pub., vol. 7, p. 462.
- Fein, J.B., Daughney, C.J., Yee, N., Davis, T.A., 1997. A chemical equilibrium model for metal adsorption onto bacterial surfaces. *Geochim. Cosmochim. Acta* 61, 3319–3328.
- Fein, J.B., Martin, A.M., Wightman, P.G., 2001. Metal adsorption onto bacterial surfaces: development of a predictive approach. *Geochim. Cosmochim. Acta* 65, 4267–4273.
- Fein, J.B., Boily, J.-F., Yee, N., Gorman-Lewis, D., Turner, B.F., 2005. Potentiometric titrations of *Bacillus subtilis* cells to low pH and a comparison of modeling approaches. *Geochim. Cosmochim. Acta* 69, 1123–1132.
- Fingler, S., Drevenkar, V., Probe, Z., 2004. Sorption of chlorophenolates in soils and aquifer and marine sediments. *Arch. Environ. Contam. Toxicol.* 48, 32–39.
- Fowle, D.A., Fein, J.B., 1999. Competitive adsorption of metal cations onto two gram positive bacteria: testing the chemical equilibrium model. *Geochim. Cosmochim. Acta* 63, 3059–3067.
- Koretsky, C., 2000. The significance of surface complexation reactions in hydrologic systems: a geochemist's perspective. *J. Hydrol.* 230, 127–171.
- Krantz-Rulcker, C., Allard, B., Schnurer, J., 1996. Adsorption of IIB-metals by three common soil fungi-comparison and assessment of importance for metal distribution in natural soil systems. *Soil Biol. Biochem.* 28, 967–975.
- Kulczycki, E., Fowle, D.A., Fortin, D., Ferris, F.G., 2005. Sorption of cadmium and lead by bacteria-ferrihydrite composites. *Geomicrobiol. J.* 22, 299–310.

- Landry, C.J., Koretsky, C.M., Lund, T.J., Schaller, M., Das, S., 2009. Surface complexation modeling of Co(II) adsorption on mixtures of hydrous ferric oxide, quartz and kaolinite. *Geochim. Cosmochim. Acta* 73, 3723–3737.
- Ledin, M., Pedersen, K., Allard, B., 1997. Effects of pH and ionic strength on the adsorption of Cs, Sr, Eu, Zn, Cd and Hg by *Pseudomonas putida*. *Water Air Soil Pollut.* 93, 367–381.
- Ledin, M., Krantz-Rulcker, C., Allard, B., 1999. Microorganisms as metal sorbents: comparison with other soil constituents in multi-compartment systems. *Soil Biol. Biochem.* 31, 1639–1648.
- Liu, A., Gonzales, R.D., 1999. Adsorption/Desorption in a system consisting of humic acid, heavy metals, and clay minerals. *J. Colloid Interface Sci.* 218, 225–232.
- Lower, S.K., Tadanier, C.J., Hochella, M.F., 2001. Dynamics of the mineral-microbe interface: use of biological force microscopy in biogeochemistry and geomicrobiology. *Geomicrobiol. J.* 18, 63–76.
- Lumsdon, D.G., 2004. Partitioning of organic carbon, aluminum and cadmium between solid and solution in soils: application of a mineral–humic particle additivity model. *Eur. J. Soil Sci.* 55, 271–285.
- Lund, T.J., Koretsky, C.M., Landry, C.J., Schaller, M.S., Das, S., 2008. Surface complexation modeling of Cu(II) adsorption on mixtures of hydrous ferric oxide and kaolinite. *Geochem. Trans.* 9, 9.
- Martell, A.E., Smith, R.M., 1977. Critical stability constants. III: Other Organic Ligands. Plenum.
- Meng, X., Letterman, R.D., 1996. Modeling cadmium and sulfate adsorption by Fe(OH)₃/SiO₂ mixed oxides. *Water Res.* 30, 2148–2154.
- Pagnanelli, F., Bornoroni, L., Moscardini, E., Toro, L., 2006. Non-electrostatic surface complexation models for protons and lead(II) sorption onto single minerals and their mixture. *Chemosphere* 63, 1063–1073.
- Schroth, B.K., Sposito, G., 1997. Surface charge properties of kaolinite. *Clays Clay Miner.* 45, 85–91.
- Schroth, B.K., Sposito, G., 1998. Effect of landfill leachate organic acids on trace metal adsorption by kaolinite. *Environ. Sci. Technol.* 32, 1404–1408.
- Serrano, S., O'Day, P.A., Vlassopoulos, D., García-González, M.T., Garrido, F., 2009. A surface complexation and ion exchange model of Pb and Cd competitive sorption on natural soils. *Geochim. Cosmochim. Acta* 73, 543–558.
- Shen, P., Huang, C., Ganguly, C., Gaboriault-Whitcomb, S., Rabideau, A.J., Van Benschoten, J.E., 2001. Comparison of soluble and immobilized acetate for removing Pb from contaminated soil. *J. Hazard. Mater.* B87, 59–72.
- Westall, J.C., 1982. FITEQL, a computer program for determination of chemical equilibrium constants from experimental data. Version 2.0. Report 82-02. Dept. of Chemistry, Oregon State Univ, Corvallis, Oregon.
- Wightman, P.G., Fein, J.B., 2005. Iron adsorption by *Bacillus subtilis* bacterial cell walls. *Chem. Geol.* 216, 177–189.
- Yee, N., Fein, J.B., 2001. Cd adsorption onto bacterial surfaces: a universal adsorption edge? *Geochim. Cosmochim. Acta* 65, 2037–2042.
- Yee, N., Fein, J.B., 2003. Quantifying metal adsorption onto bacteria mixtures: a test and application of the surface complexation model. *Geomicrobiol. J.* 20, 43–60.
- Zachara, J.M., Resch, C.T., Smith, S.C., 1994. Influence of humic substances on Co²⁺ sorption by a subsurface mineral separate and its mineralogical components. *Geochim. Cosmochim. Acta* 58, 553–566.